Effects of Enhanced Image Quality in Infrastructure Monitoring through Micro Aerial Vehicle Stabilization

Chung-Hsin Kuo, Sébastien Kanlanjan, Louis Pagès, Hanadi Menzel, Sascha Power, Chen-Ming Kuo, Christian Boller, Sébastien Grondel

7th European Workshop on Structural Health Monitoring
July 8-11, 2014. La Cité, Nantes, France

EFFECTS OF ENHANCED IMAGE QUALITY IN INFRASTRUCTURE MONITORING THROUGH MICRO AERIAL VEHICLE STABILIZATION

Chung-Hsin Kuo[1], Sébastien Kanlanjan[3], Louis Pagès[3], Hanadi Menzel[1], Sasha Power[1], Chen-Ming Kuo[1], Christian Boller[1,2] and Sébastien Grondel[3]
[1]*Chair in NDT & QA (LZfPQ), University of Saarland, Saarbrücken, Germany*
[2]*Fraunhofer IZFP, Saarbrücken/Germany*
[3] *Université de Valenciennes, Valenciennes, France*

c.boller@mx.uni-saarland.de

ABSTRACT

Traditional monitoring of large infrastructure such as towers of churches or for cooling, chimneys or any other type of tall buildings can require extreme effort and hence become very risky and costly since it mainly requires people to be moved around. An interesting alternative in that regard is the use of rotary wing micro aerial vehicles (MAV) equipped with sensors such as digital cameras to capture series of images and stitch them on to a 3D model. However the images recorded always have "noise" which is caused by the vehicle movement during the inspection process. Experiments have been carried out using a multi-rotor copter with an off the shelf camera for building inspection (aerial photography) for years [1]. To validate the effect of MAV flight stabilization a vector thrust principle recently developed at Saarland University (patent application in progress [18]) has been implemented onto a MAV for flight stabilization. The paper describes the procedure of MAV-based infrastructure monitoring as well as the image stitching process in general before explaining the vector thrust design principle and the enhancements achieved in terms of image resolution and processing.

INTRODUCTION

An increasing amount of civil infrastructure buildings (including roads and bridges) has become an issue with regard to the ageing process and hence a resulting case for life cycle management. According to the Federal Highway Administration (FHWA), nearly 70% of all bridges and roads need to be inspected regularly in the USA [2, 3, 4, 5, 6]. This inspection is based on purely visual methods and is completed by inspection personnel present on site [7, 8, 9]. However, apart from bridges, there is a large amount of other infrastructure such as public buildings, industrial sites or even cultural heritage where condition monitoring and life cycle management is still much less from being established. Inspecting various of this infrastructure can be dangerous for inspectors to be on site, as some locations on the structure may only be accessed under extreme circumstances, such as very slender, high towers [10, 11, 12, 13]. Since most inspections refer to visual inspection (around 95%), a robot equipped with a digital camera instead of a human inspector looks to be an option of much lower risk. A multi-rotor copter (in this case an octocopter) generally considered as a micro aerial vehicle (MAV) is a fairly popular solution and was hence used throughout this project, as it offers sufficient payload capacity, is small in size, and most importantly is comparatively simple with regard to the mechanical structure. (Fig. 1)

This type of aerial inspection includes two major parts, collecting data using a camera on board and processing the data collected. The infrastructures' façades of interest are scanned by the MAV floor by floor by capturing images that are then verified and stitched together. This image stitching has been initially done using an image processing software such as Photoshop to form an overview for each façade where

more sophisticated tools and algorithms to allow for automated image stitching are currently explored.

Diameter	1.02 m
Take-Off Weight	2.5 kg
Endurance	< 20 min
Max. Payload	2 kg

Figure 1: Octocopter used and technical data

The first inspection mission took place at the Fraunhofer IZFP building in Saarbrücken/Germany where the rendered line in Fig. 2 shows the area monitored. The reason why not all of the building has been monitored results from the fact that trees have been close to the remaining parts of the building which avoided images to be taken by a flying vehicle. The total inspection took less than 8hrs including time for the actual flight and photo checking with images recorded having a resolution that allows cracks to be clearly determined down to around 10 millimetres in size. Compared to a conventional inspection this is easily an increase in inspection performance by a factor of four to five. The images collected were processed to form an overall map of each façade which were then further combined to a 3D model for further visualization (Fig.3).

Figure 2: Left: Aerial view of Fraunhofer IZFP building with rendered line indicating inspection facade. Right: Front view of the Fraunhofer IZFP building.

There was around 4GB of photo material collected for each façade of the building. However, only around 10% of the photos were selected for the image processing in the end. The rest was not usable due to the large amount of attitude noise (roll, pitch and yaw angle) which leads to image distortion. A selection of photos taken is shown in Fig. 4 where a strong variation in attitude can be recognized even though a gimbaled attitude stabilization system had already been used for the camera system.

It becomes apparent that an enhancement in stabilization of the monitoring vehicle will enhance the percentage of images useful for the image stitching process which again enhances the monitoring process in terms of inspection time and hence cost. A means on how to further stabilize the MAV is therefore described and discussed along the paragraphs to follow.

VECTOR THRUST PROPULSION FOR ROTORCRAFT MAV ATTITUDE NOISE REDUCTION

Traditionally for a multi-rotor copter to perform any translation in x or y direction will require attitude change [14, 15, 16] which is achieved through displacement control resulting from a difference of the motors' rotational speed. (Fig. 5)

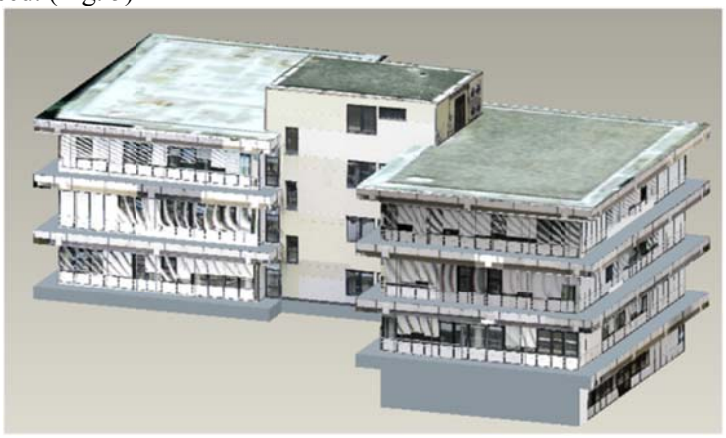

Figure 3: 3D CAD model of inspected building (Fraunhofer IZFP)

Figure 4: Selection of photos taken as an example to show variation in attitude

This attitude change is the main source of noise during an image capturing process (even with a camera gimbal stabilization the attitude change still has a significant effect). However, translation in any x, y and z direction is required for the MAV along a building inspection. In order to have the translation and stabilization of the image at same time, a vector thrust system is proposed for a multi-rotor copter, which will be explained on a quadcopter here as an example but which in principle can be applied to any even number of rotors vehicle in general.

The concept of vector thrust is based on directing thrust to a desired direction instead of using attitude change of the vehicle to generate an x or y translation. Fig. 5 shows the force and torque diagram of the quadrocopter where the axis system in the diagram is set to be a "plus" frame system (where x and y axis is along vehicle's arm) [1].

A plus frame configuration is simple to construct both mathematically and mechanically. However, Kuo and Boller [17] have shown that a plus frame with vector thrust will create an unwanted yaw moment that can be corrected by setting a heading lock on the controller but is still not really acceptable for an inspection purpose. On the other hand, an X configuration, where the axes are rotated 45 degrees in anti-clock

wise direction, the vector thrust does not create the unwanted yaw moment during flight which can be explained from the set of equations described below.

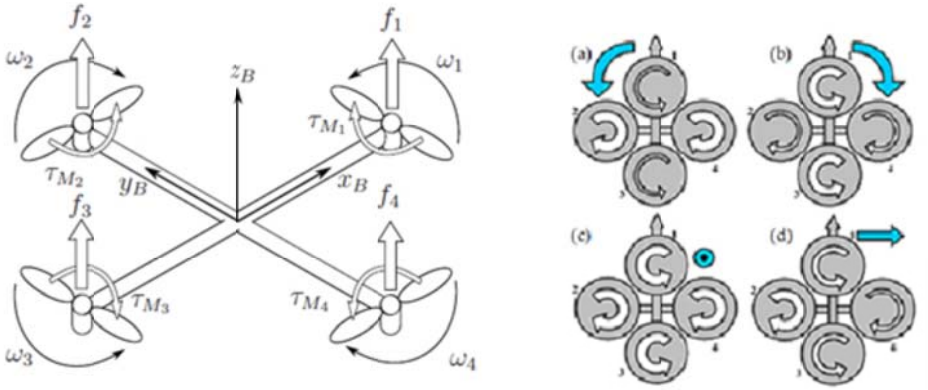

Figure 5: Left: Free force diagram of the multi-rotor robot (quad). Right: Motion diagram, a) yaw anti-clockwise, b) yaw clockwise, c) increase altitude (movement in z direction only), d) roll positive to create motion in y direction.

For the X configuration the relationship between force and torque and the motor rotating speed in each axis is as follows:

$$F_x = -b(\varpi_1^2 + \varpi_2^2 + \varpi_3^2 + \varpi_4^2)\sin\theta_s$$

$$F_y = b(\varpi_1^2 + \varpi_2^2 + \varpi_3^2 + \varpi_4^2)\sin\phi_s$$

$$F_z = b(\varpi_1^2 + \varpi_2^2 + \varpi_3^2 + \varpi_4^2)\cos|\theta_s|\cos|\phi_s| \quad (1)$$

$$\tau_\phi = (F_{1Z} + F_{2Z} - F_{3Z} - F_{4Z})l\cos 45 + (\tau_1 + \tau_2 + \tau_3 + \tau_4)\sin\theta_s$$

$$\tau_\theta = (F_{2Z} + F_{3Z} - F_{1Z} - F_{4Z})l\cos 45 + (\tau_1 + \tau_2 + \tau_3 + \tau_4)\sin\phi_s$$

$$\tau_\psi = (\tau_1 + \tau_2 + \tau_3 + \tau_4)\cos|\phi_s|\cos|\theta_s| \quad (2)$$

By combination of (1) and (2) a 6 DOF equation can be constructed which is shown in (3)

$$\begin{pmatrix} \frac{F_x c\theta c\psi + F_y c\theta s\psi - F_z s\theta}{m} \\ \frac{F_x(s\phi s\theta c\psi - c\phi s\psi) + F_y(s\phi s\theta s\psi + c\phi c\psi) + F_z s\phi c\theta}{m} \\ \frac{F_x(c\phi s\theta c\psi - s\phi s\psi) + F_y(c\phi s\theta s\psi - s\phi c\psi) + F_z c\phi c\theta}{m} - g \\ \frac{(b(\varpi_1^2+\varpi_2^2-\varpi_3^2-\varpi_4^2)\cos\theta_s\cos\phi_s)l\cos 45 - d(\varpi_2^2+\varpi_4^2-\varpi_1^2-\varpi_3^2)\sin\theta_s - \dot{I}_{xx}\dot{\phi})}{I_{xx}} \\ \frac{(b(\varpi_3^2+\varpi_2^2-\varpi_1^2-\varpi_4^2)\cos\theta_s\cos\phi_s)l\cos 45 - d(\varpi_2^2+\varpi_4^2-\varpi_1^2-\varpi_3^2)\sin\phi_s - \dot{I}_{yy}\dot{\theta})}{I_{yy}} \\ \frac{d(\varpi_1^2+\varpi_2^2+\varpi_3^2+\varpi_4^2)\cos\theta_s\cos\phi_s - \dot{I}_{zz}\dot{\psi}}{I_{zz}} \end{pmatrix} = \begin{pmatrix} \ddot{x} \\ \ddot{y} \\ \ddot{z} \\ \ddot{\phi} \\ \ddot{\theta} \\ \ddot{\psi} \end{pmatrix} \quad (3)$$

Where:

q = 6 DOF generalized vector
τ = Torque
F_x, F_y, F_z = force in x, y and z direction (body axis)
ϖ = rotational speed of motor i
ϕ, θ, ψ = Roll, pitch and yaw angle (attitude)
$c\phi, \theta, \psi . s\phi, \theta, \psi = \cos\phi$ or θ or $\psi . \sin\phi$ or θ or ψ
b = Lift constant
d = Drag constant

Since the vehicle is at near hover condition, $\dot{I}_{xx}\dot{\phi}$, $\dot{I}_{yy}\dot{\theta}$ and $\dot{I}_{zz}\dot{\psi}$ are assume to be zero.

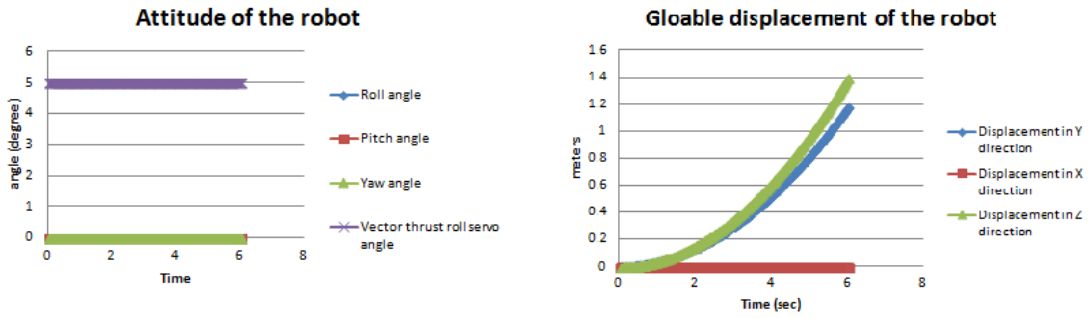

Figure 6: **Left**: Numerical simulation results of MAV (robot) attitude when vector thrust roll servo is active at 5 degree. (Note: no autopilot control). **Right**: global displacement of the robot. Note: no undesired x displacement due to no yaw angle created.

Results from numerical simulations displayed in Fig. 6 show that vector thrust is active for y direction, and that there is no undesired roll, pitch and yaw angle during y direction movement (vehicle moves along an axis without any attitude change). This vector thrust approach has been applied for a European patent [18].

VECTOR THRUST IMPLEMENTATION

Both hard- and software modifications have to be made in order to apply the vector thrust system onto an ordinary quadcopter. Hardware-wise extra mechanical joints have to be implemented to allow rotation of the motors (thrust) to operate into the desired direction. The joint system is not allowed to be too heavy but at the same time needs to have enough strength to withstand the twisting moment of the thrust and vibrations from the motor.

There are already off the shelf components available for fixed wing vector thrust designs (Fig. 7, left), designed originally for small fixed wing aircraft. However those are not sufficient in strength and fracture easily (Fig. 7 right).

The joint was redesigned with enhanced supporting points and linked to a servo that changes the angles to achieve the vector thrust feature (Fig. 8).

Software-wise a new control loop has to be implemented to adapt to the vector thrust flying mode. For easy use and proof of concept, control software has been designed to allow the pilot to switch from normal flight mode to vector thrust flight mode by one switch even during flight. Various frame designs for

the vehicle were tested and the approach of only implementing vector thrust in x-direction was taken due to complexity of the mechanical system.

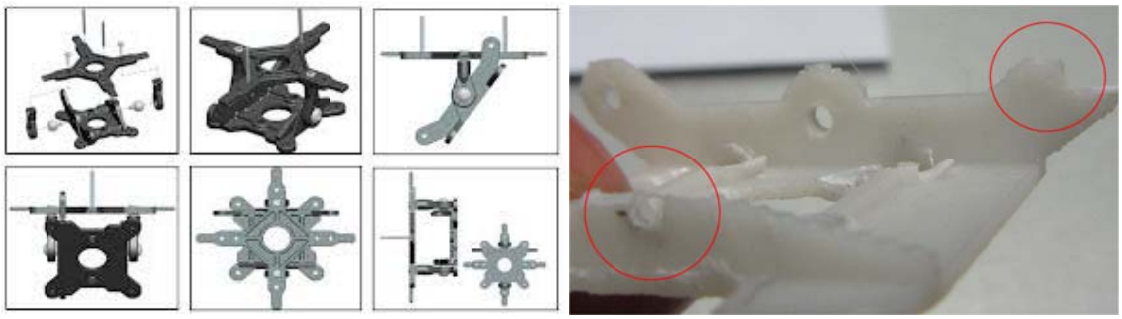

Figure 7 **Left**: Off the shelf vector thrust joint. **Right**: Weak contact points (circles)

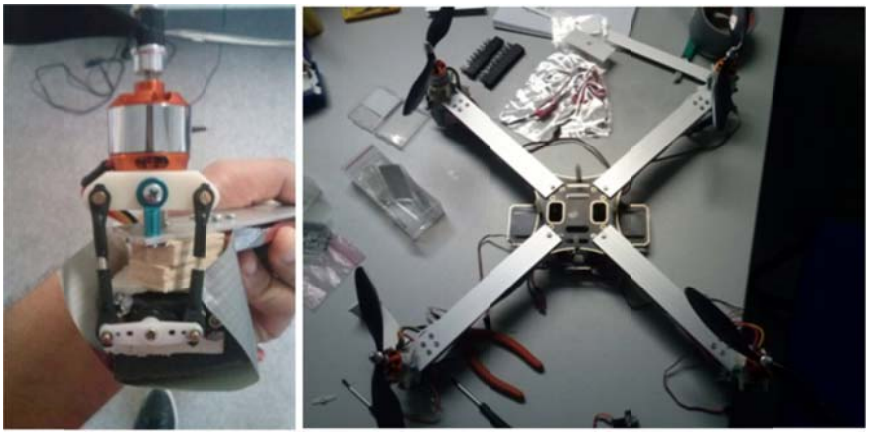

Figure 8 Left: Vector thrust enabled motor.
Right: All system shown on the left is implemented to all four motors on board.

Figure 9: Vector thrust motor operating. Lines indicate the motor angle.

FLIGHT RESULTS

In order to have a fair flight test to demonstrate the capabilities of the vector thrust concept, the control system has been modified to allow for both "normal" and "vector thrust" flight mode. Fig. 10 shows the attitude reading from the flight where the lighter (red) line indicates the actual roll angle and the black line indicates the input signal from pilot command (roll angle in this case). "Normal" flight is the region in the left hand rendered box, where the large roll angle can be seen when pilot applies a roll (side way) displacement command. However, the performance becomes completely different and hence stable once the copter enters into the vector thrust mode. The roll angle in the right hand rendered box (vector thrust mode) stays at a minimum when the pilot gives a side way (roll) command, which means the vehicle is moving sideways without any attitude change, becoming much more stable with a significant improvement of the image captured.

Fig. 11 shows the comparison of images captured in normal (left) and vector thrust (right) mode and the resulting stitched image can be seen in Fig.s12 and 13. Note that the vector thrust mode not just generates better images but also allows for fewer images to be taken for stitching the complete image resulting in an improvement of the MAV's data storage capacity. A comparison of the number of images required shows that a third less was required.

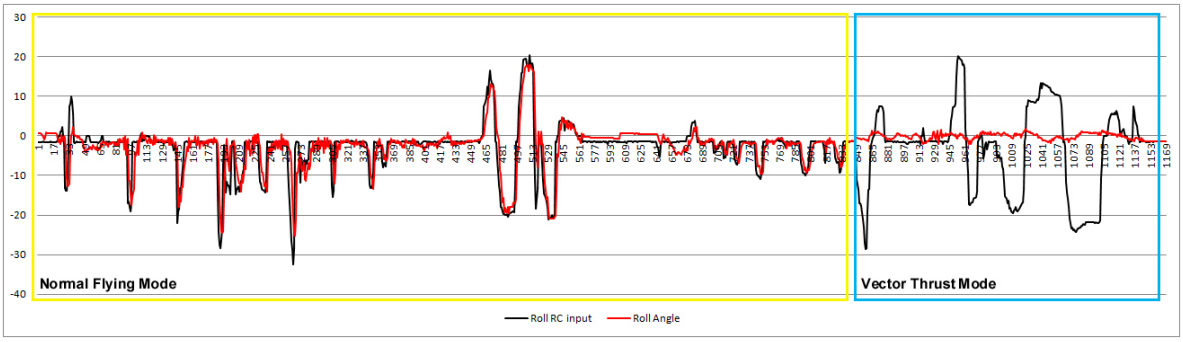

Figure 10: On board accelerometer roll reading (black) and RC roll input (red/light)

Fig. 11 **Left**: Normal flying mode **Right**: Vector thrust mode
Note: The images are tilted in normal flying mode

Figure 12: Stitched image from normal flying mode (6 images used)

Figure 13: Stitched image from vector thrust mode (4 images used)

CONCLUSION AND FUTURE WORK

The motion simulation and flight results show that the vector thrust concept results in a significant improvement of the attitude control for a multi-rotor copter (here a quad) in use of photographic inspection. It can be concluded that this advantage also exists when other types of sensors are applied which will even allow to look below a structure's surface such as when using thermography or radar. However, a vector thrust system requires additional mechanical parts which lead to a weight increase that can become an issue. A means of compensation in that regard is the number of rotors that may be increased and the structural complexity to be reduced being aspects to be considered with future developments.

REFERENCES

[1] C.-H. Kuo, A. Leber, C.-M. Kuo, C. Boller, C. Eschmann and J. Kurz. Unmanned robot system for Structure health monitoring and Non-Destructive Building Inspection, current technologies overview and future improvements; Proc. of the Internat. Workshop on SHM, Stanford Univ., Stanford/CA, USA, September 2013

[2] Golabi K, Thompson P, Hyman W. Pontis. A network optimization system for bridge improvements and maintenance Technical manual. Publication number FHWA-SA-94-031: US Department of Transportation, Federal Highway Administration; 1993.

[3] Brecher A.. Infrastructure: a national priority. Soc Women Eng 1995; 4(16):14-16.

[4] Roberts E, Shepard R.. Bridge management for the 21st century. Transport Res Rec 2000;1696:197-203.

[5] Bridge Inspection Robot Development Interface (BIRDI). Development of high-tech automatic robot system for bridge inspection and monitoring, Technical report for Ministry of Construction and Transportation (in Korean), 2007.

[6] Federal Emergency Management Agency (FEMA). Module 1C structural engineering, structural collapse technician course - student manual 8 http://www.fema.gov/emergency/usr/sctc.shtm20098 (last visit Dec, 2009)

[7] Aldunate R., S.F. Ochoa, F. Pena-Mora, M. Nussbaum. Robust mobile ad hoc space for collaboration to support disaster relief e_orts involving critical physical infrastructure, Journal of Computing in Civil Engineering 20 (1) (2006) 13-27.

[8] Federal Highway Administration (FHWA). Bridge Inspections Training Manual, July 1991.

[9] Bridge Maintenance Training Manual. US Federal Highway Administration, FHWAHI-94-034, Prepared by Wilbur Smith Associates, 1992.

[10] NJDOT, Bridge Inspection Work Zone. Setup Guide, 2009. http://www.state.nj.us/

[11] Shibata T. and A. Shibata. Summary report of research and study on robot systems for maintenance of highways and bridges, Robot, vol. 118, JARA, Tokyo, Japan, Sep. 1997, pp. 41-51.

[12] Product Catalog. Paxton-Mitchell Snooper? Series 140 http://www.paxtonmitchell.com

[13] Oh J.-K., A.-Y. Lee, S.M. Oh, Y. Choi, B.-J. Yi, H.W. Yang. Design and control of bridge inspection robot system, IEEE Int. Conf. on Mechatronics and Automation, Aug. 2007, pp. 3634-3639.

[14] Luukkonen T. Modelling and control of quadcopter; School of Science. Independent research project in applied mathematics Espoo, August 22, 2011. Aalto University.

[15] Group 10833. "Modelling and Control of Autonomous Quad-Rotor". 2nd Semester Project of the Intelligent Autonomous Systems Master Programme Faculty of Engineering, Science and Medicine. University of Aalborg, Denmark June 2010.

[16] Naidoo Y., R. Stopforth and G. Bright. Quad-Rotor Unmanned Aerial Vehicle Helicopter Modelling & Control; Intech open access publisher. Aug 2011

[17] C.-H. Kuo, C.-M. Kuo, A. Leber and C. Boller. Vector thrust multi-rotor copter and its application for building inspection. IMAV2013 Toulouse, France

[18] European Patent Office, Submission number: 2288267, Application: EP13183347.7, Reference Code: F54634-EP